EXPERIMENTAL AND NUMERICAL STUDY OF THE EFFECT OF THE PRESENCE OF A GEOMETRIC DISCONTINUITY OF VARIABLE SHAPE ON THE TENSILE STRENGTH OF AN EPOXY POLYMER

Khalissa SAADA*,, Salah AMROUNE*,**, Moussa ZAOUI*,**
Amin HOUARI***, Kouider MADANI***, Amina HACHAICHI******

*Department of Mechanical Engineering, University of Mohamed Boudiaf-M'Sila, M'sila, Algeria
**Laboratoire de Matériaux et Mécanique des Structures (LMMS), Université de M'sila, M'sila, Algérie
***Laboratoire de Matériaux, et Mécanique des Structures (LMMS), Université SBA. Sidi Bel Abesse, Algérie
**** Faculty of Technology, M'hamed Bougara, University, Boumerdes 35000, Algeria

khalissa.saada@univ-msila.dz, salah.amroune@univ-msila.dz, moussa.zaoui@univ-msila.dz
houari.latif2016@gmail.com, koumad10@yahoo.fr, a.hachaichi@univ-boumerdes.dz

received 25 October 2022, revised 2 January 2023, accepted 2 January 2023

Abstract: The presence of geometric discontinuity in a material reduces considerably its resistance to mechanical stresses, therefore reducing the service life of materials. The analysis of structural behaviour in the presence of geometric discontinuities is important to ensure the proper use, especially if it is regarding a material of weak mechanical properties such as a polymer. The objective of the present work is to analyse the effect of the notch presence of variable geometric shapes on the tensile strength of epoxy-type polymer specimens. A series of tensile tests were carried out on standardised specimens, taking into account the presence or absence of a notch. Each series of tests contains five specimens. Two notch shapes were considered: circular (hole) and elliptical. The experimental results in terms of stress–strain clearly show that the presence of notches reduces considerably the resistance of the material, where the maximum stress for the undamaged specimen was 41.22 MPa and the lowest stress for the elliptical-notched specimen was 11.21 MPa. A numerical analysis by the extended finite element method (XFEM) was undertaken on the same geometric models; in addition, the results in stress–strain form were validated with the experimental results. A remarkable improvement was obtained (generally an error within 0.06%) for strain, maximum stress, Young's modulus and elongation values. An exponential decrease was noted in the stress, strain, and Young's modulus in the presence of a notch in the material.

Key words: Tensile test, Hole-notched, Elliptical-notched, XFEM, Finite element method

1. INTRODUCTION

In the recent years, scientific researchers and industrial experts have focused their efforts on biocomposite materials, due to their properties of being sustainable, renewable, biodegradable and biocompatible [1-4]. Biocomposite materials can be used in different areas of applications, especially in light structures that have a bolted assembly before using. It is necessary to determine their mechanical properties through the different experimental techniques used under different types of loading such as traction [5–7], compression [8, 9], torsion [10–12], fatigue [13–15] and impact [16]. The study of the geometry effect of the tensile specimens on the mechanical properties has gained importance from several authors. Notably, Baykan et al. [17] conducted an experimental study on the effect of hole size and position on the mechanical properties of tensile specimens using peridynamic (PD) theory and compared them numerically using code developed on MATLAB and ANSYS. The authors noticed that PD can accurately capture fracture stress, strain and hole interaction in composite laminates.

In another study presented by Hao et al. [18], plastic specimens reinforced with Kenaf fibres containing holes of different diameters were produced. These specimens were tested in uniaxial tensile, open hole tensile, tension at different strain rates, bending and in-plane shear. The obtained results indicated that those treated at a higher temperature of 230°C, but at a shorter time of 60 s, had the best mechanical performance. Also, the linear elastic finite element (FE) model of KPNCs agreed well with the experimental results in the valid strain range of 0%–0.5% for the uniaxial tensile test and 0%–1% for the bending test. Tensile specimens according to ASTM D1822 were manufactured using a 3D printer by Galeta et al. [19]. In this study, the authors determined the impact of three different lattice-like hollow structures considered as honeycombs, drills and scratches on the tensile strength of 3D printed samples. The test samples were prepared on a 3D printer, with variations of the geometric structure internal. The results of the tensile test revealed that the honeycomb structure and the structured samples exhibited the greatest strength.

Khosravani et al. [20] found that the tensile strength of samples of polylactic acid (PLA) and acrylonitrile butadiene styrene (ABS) indicates that increasing the diameter of the hole leads to a decrease in the strength of the part. The finite element method (FEM) has been generally used for predicting the mechanical behaviour of composite materials [21–23], while Mohammadi et al. [24] established standard open-hole tensile (OHT) laminated

composites using the FEM to quantify the damage mechanism. Moreover, Ghezzo–Fabrizia et al. [25] presented a numerical and experimental study conducted on T300/epoxy carbon fibre thin laminates with multiple cutouts subjected to in-plane loads. Liao and Adanur [26] studied a new model, which is based on the geometric modelling of woven and braided fabric structures in three dimensions using a computer-aided geometric design (CAD) technique. Recently, Recement Bogrekci et al. [27] analysed the impact of modified PLA specimen geometries on structural strength using FE analysis. Moreover, several types of adhesives such as epoxy, polyester resin, phenolic and polyurethane have been used for manufacturing of sandwich joints [28, 29].

Most of these studies did not take into account in their analysis the effect of the presence of notches on a material with weak mechanical properties such as polymer. Our work is a part of this context. The aim of this paper is to propose a mixed extended finite element method (XFEM) formulation for the elasto-plastic analysis of stress and strain. The objective is to see the effect of the presence of a geometric discontinuity on the tensile strength of an epoxy type-polymer and to see how its mechanical properties evolve compared with the shape of the notch, and on the other hand, to try to use the XFEM to analyse the variation of the stress applied according to the deformation. Tensile tests were carried out on specimens in the presence of different shapes of geometric discontinuity (hole, elliptical notch). The effect of these geometric shapes (hole and ellipse) on the mechanical properties of the polymer was examined and compared with undamaged specimens. The experimental results were compared with those obtained with the FE numerical analysis using the ABAQUS software using XFEM. The effect of the geometric shape of the notch was evaluated in terms of the maximum stress and maximum deformation. On the other hand, the calculation of the stress concentration factor K_t in the different epoxy specimens has been highlighted.

2. MATERIALS AND METHODS

2.1. Specimen geometry

The epoxy polymer specimens intended for the tensile test are shown in Fig. 1. The dimensions are standardised according to the ASTM D638-14 standard (Fig. 1a). Two notch shapes were considered: a circular shape (Fig. 1b) and an elliptical shape (Fig. 1c). The presence of the notch aims to concentrate the stresses and locate a plastification, which will be a source of initiation of the damage.

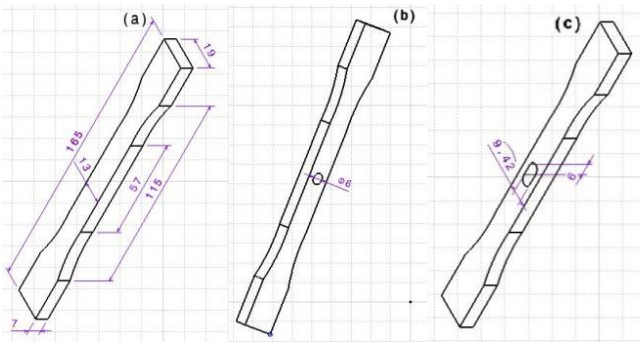

Fig 1. (a) Undamaged specimen, (b) specimen with hole and (c) specimen with elliptical notch

The dimensions of the samples were 165 × 19 × 7 mm3, where the hole diameter is about 6 mm and for the elliptical notch the dimensions are r^1 = 3 mm, r^2 = 6 mm.

2.2. Test procedure

The samples were connected to the handles of the device and then the displacement was measured by the computer program. The stress values relate to the force (F) and section area (S) of samples. Also, the force–displacement curves of the samples are recorded followed by incorporation of the total energy absorption (EA) into the force–displacement curve with the following relation [30]:

$$EA = \int_0^S FdS = F_m S \tag{1}$$

For displacement u and field q to be used for the XFEM of the model [31].

$$U^h = \sum_{i\in\mathcal{M}} N_i u_i^{(\mathcal{M})} + \sum_{i\in\mathcal{H}} \widetilde{N}_i H u_i^{\mathcal{H}} + \sum_{i\in\mathcal{K}} \sum_{j=1}^{4} \widetilde{N}_i F_j^{(u)} u_{ij}^{(\mathcal{K})} = H\hat{u} \tag{2}$$

$$\mathrm{q}^{\mathrm{h}} = \sum_{\mathrm{i}\in\mathcal{M}} \mathrm{N_i q_i^{\mathcal{M}}} + \sum_{i\in\mathcal{H}} \widetilde{N}_i H q_i^{\mathcal{H}} + \sum_{i\in\mathcal{K}} \sum_{j=1}^{2} \widetilde{N}_i F_j^{(q)} q_{ij}^{(\mathcal{K})} = H_q \hat{q} \tag{3}$$

where: i and j are a numbered node, $\hat{\mathrm{u}}$, $\hat{\mathrm{q}}$ are the global vectors, and $\mathrm{N_i}$ corresponds to the functions of quadratic shape approximation or associated with the linear continuum, while $\widetilde{\mathrm{N}}_\mathrm{i}$ is the linear shape function of the FEs which construct the partition of unity. $\mathrm{u_i^{(\mathcal{M})}}$, $\mathrm{u_i^{\mathcal{H}}}$, $\mathrm{q_i^{\mathcal{M}}}$, $\mathrm{u_{ij}^{(\mathcal{K})}}$, $\mathrm{q_i^{\mathcal{H}}}$ and $\mathrm{q_{ij}^{(\mathcal{K})}}$ denote the unknowns at i, H and $\mathrm{F_j^{(q)}}$ are the functions on the sides.

In this work, we used the XFEM technique which allows us to initiate and predict the propagation of the crack in the structure to be damaged. Our structure is fixed in their extremities in order to quickly cause the damage, adding to this the mode of loading that appears as an important effect and quickly causes the damage in our analysis. Not only does it accumulate the load to quickly cause the damage, but it also gives us a broad understanding of the behaviour of our structure for analysis. The XFEM technique is implemented in the standard ABAQUS calculation code. In technique XFEM the damage is presented in the following forms:

$$u(x) = \sum_{i=N} N_i(x) u_i + \sum_{i\in N_d} N_i(x) H(x) a_i + \sum_{i\in N_p} N_i(x) \left(\sum_{j=1}^{4} F_i(x) b_i^j\right) \tag{4}$$

where N is all the nodes of the mesh and u_i is the classical degree of freedom at node I; $N_{\_i}$ (x) are the classical FE shape function associated with node I, where a and b are the corresponding degrees of freedom, H(x) is a Heaviside type enrichment function and $\mathrm{F_i(x)}$ Enrichment functions represent the singularity in the vicinity of the crack front as follows:

$$\{F_i(x)\} = \left\{\sqrt{r}sin\frac{\theta}{2}, \sqrt{r}cos\frac{\theta}{2}, \sqrt{r}sin\frac{\theta}{2}sin\frac{\theta}{2}, \sqrt{r}cos\frac{\theta}{2}sin\frac{\theta}{2}\right\} \tag{5}$$

In the deformation zone, there is a point (yield point) which, if exceeded by the stress value, does not return to its original value [32] as follows:

$$\sigma = \sigma_e(1+\varepsilon) \tag{6}$$

$$\int_0^{\varepsilon} d\varepsilon = \int_{l_0}^{l_i} \frac{dl}{l} \tag{7}$$

$$\varepsilon_{true} = ln\left(\frac{l_i}{l_0}\right) \quad (8)$$

$$\varepsilon_{true} = ln\left(\frac{l_0+\Delta l}{l_0}\right) \quad (9)$$

$$\varepsilon_{true} = ln(1+\varepsilon) \quad (10)$$

Isotropic materials have the same mechanical properties in all directions in all points of the material as follows:

$$\begin{bmatrix}\sigma_1\\ \sigma_2\\ \sigma_3\\ \sigma_4\\ \sigma_5\\ \sigma_6\end{bmatrix} = \begin{bmatrix} C_{11} & C_{12} & C_{13} & 0 & 0 & 0\\ & C_{11} & 0 & 0 & 0 & 0\\ & & C_{11} & 0 & 0 & 0\\ & & & \frac{C_{11}-C_{12}}{2} & 0 & 0\\ & & & & \frac{C_{11}-C_{12}}{2} & 0\\ & \text{sym} & & & & \frac{C_{11}-C_{12}}{2}\end{bmatrix}\begin{bmatrix}\varepsilon_1\\ \varepsilon_2\\ \varepsilon_3\\ \varepsilon_4\\ \varepsilon_5\\ \varepsilon_6\end{bmatrix} \quad (11)$$

For the ellipse shape which is parallel to the axis and the plate α = 0 or α = π/2, which indicated the concentration of stresses around the ellipse and the concentration of stress at the edge of the given hole [33]:

$$\bar{\sigma} = \sigma^{\infty}\frac{1-m^2-2m+2\cos 2\theta}{1-2m\cos 2\theta+m^2} \quad (12)$$

so that $0 \leq m \leq 1$.

The maximum stress equals:

$$\sigma_{max} = k_t\sigma_{nom} \quad (13)$$

The stress concentration factor kt:

$$k_t = 1 + 2\sqrt{\frac{a}{R}} \quad (14)$$

R: Curve radius

2.3. Materials tested

Three sample types of epoxy resin with and without fibres were prepared, and the notches were created in the shape of elliptical holes (Fig. 2). During the manufacturing process, the samples were exposed to a polymerisation temperature of 70° and for 5 h in order to improve their mechanical properties. The testing conditions were as follows: these samples will be subjected to a tensile test under a displacement speed estimated at F = 1 mm/min and the diameter of the hole was droll = 6 mm for hole-notched specimen and the dimensions of the samples were 165 × 19 × 7 mm^3.

2.4. Design of experiments

The purpose of determining the tensile curves for the different specimens was to take into account the location of rupture of the specimens by the presence of notches. The different geometric notch shapes have the purpose of defining the sensitivity of the specimen with respect to the tensile loading. For this, five specimens were considered for each type, as shown in Fig. 2.

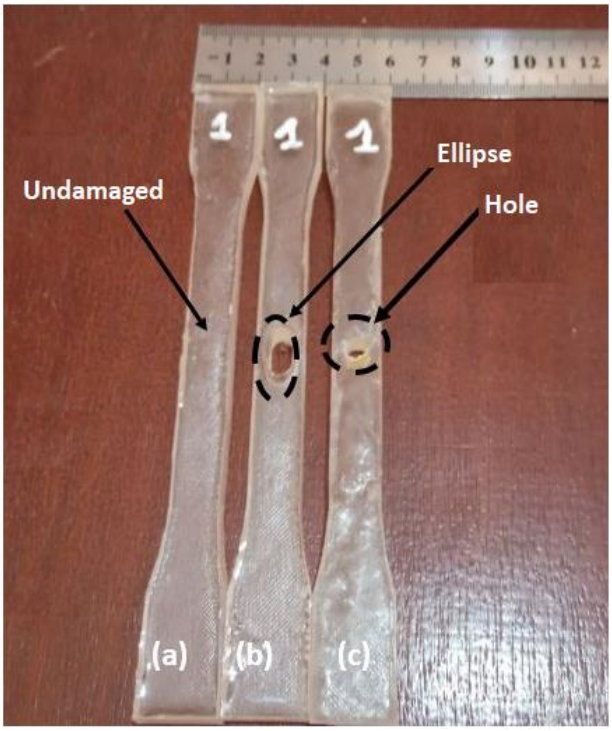

Fig. 2. (a) The undamaged sample of epoxy. (b) Epoxy specimens with ellipse. (c) Epoxy specimens with hole

3. EXPERIMENTAL ANALYSIS

The experimental results obtained refer to five samples for each of the specimens: complete Fig. 3(a), hole-notched specimen Fig. 3(b) and elliptical-notched specimen Fig. 3(c). Obtaining a reproducibility of the results was a little difficult, especially for the samples in the presence of elliptical notch. Machining this shape was a bit difficult. For the other specimens the shape of the curves was the same. We notice a variation in the tensile curves for the three specimens, where the mechanical properties of resistance (stress and Young's modulus) as well as the deformation were influenced by the presence of notches. A considerable drop in these properties is noted compared with the results of the solid samples (Fig. 4). The maximum stress is dropped from 40 MPa to 21.06 MPa (a reduction of almost 50%) for the samples with holes and 11.21 MPa (a reduction of almost 75%) for the samples with elliptical notch.

The experimental results in Fig. 4, including Young's modulus and maximum stress value, indicate that the highest value for them is at the undamaged specimen (1,793.80 MPa and 41.22 MPa, respectively). The value of the hole-notched specimen is lower with a Young's modulus of 1,423.36 MPa and a maximum stress equal to 21.06 MPa; the smallest of them is the elliptical-notched specimen with a maximum stress of 11.21 MPa and a Young's modulus of 547.59 MPa.

The experimental results indicate that the elasticity area of the undamaged specimen is larger than the elasticity area of the hole-notched specimen and the elliptical-notched specimen.

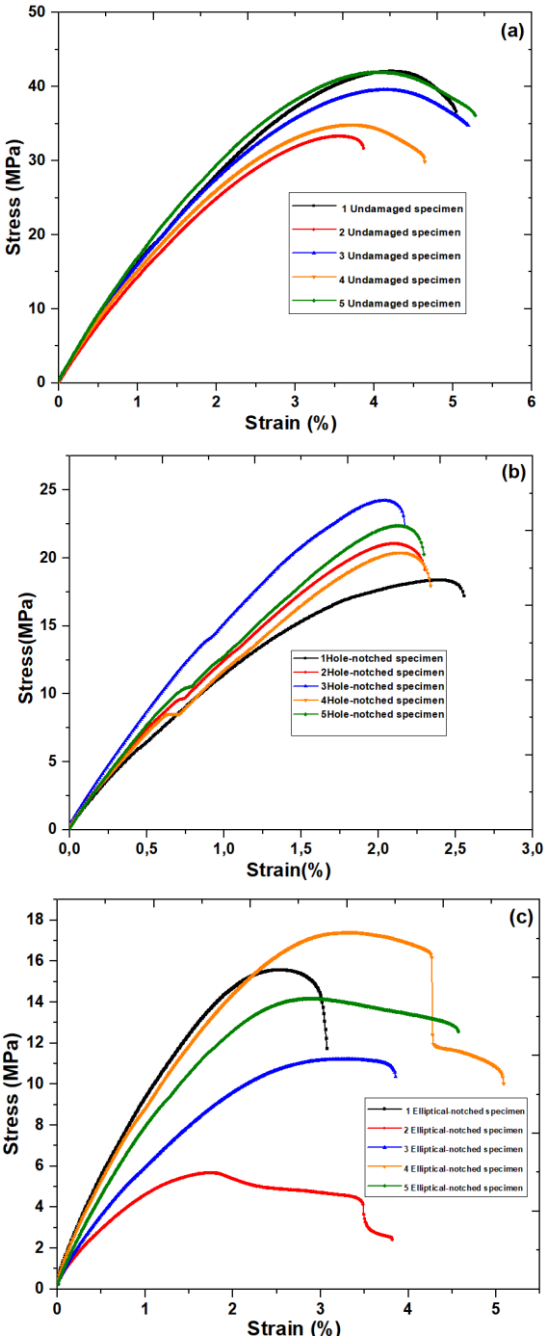

Fig. 3. Different experimental results for the five samples. (a) The five undamaged specimens. (b) The five hole-notched specimen. (c) The five elliptical-notched specimens

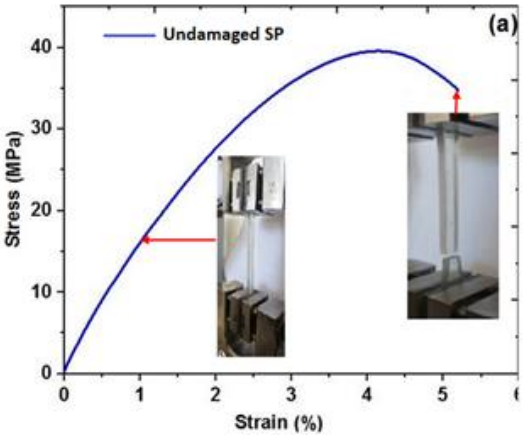

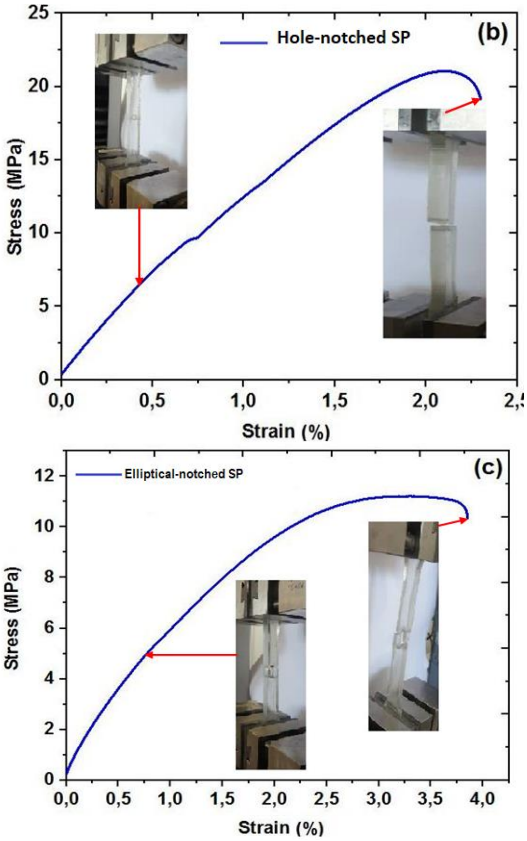

Fig. 4. Comparison of the experimental results of the mean of the three specimens: (a) The undamaged sample. (b) The hole-notched specimen. (c) The elliptical-notched specimen

3.1. Analysis of tensile test specimens

The three-epoxy specimens were analysed by performing a (Fig. 4) tensile test to obtain the mechanical properties and entering the values for numerical analysis using the Abaqus program; the results are shown in Tab. 1.

Tab. 1. Mechanical properties of Epoxy specimen under tensile test

Features	Young's modulus (MPa)	ε-Fmax (%)	εBreak (%)	σBreak (MPa)	Maximal stress (MPa)
Undamaged specimen	1,793.80	4.12	5.19	34.74	39.58
Hole-notched specimen	1,423.36	2.11	2.30	19.15	21.06
Elliptical-notched specimen	547.59	3.30	3.86	10.36	11.21

Fig. 5 summarises the tensile test results for the three epoxy samples, where the results of standard deviation showed the effect of the samples on the mechanical properties. We notice that the larger the hole opening like ellipse, the lower the results of stress and Young's modulus, as well as strain. We also notice a convergence between the strain results for each of the hole-notched specimen and elliptical-notched specimens.

The three test samples for the undamaged specimen and the hole-notched specimen as well as the specimen containing the ellipse shape had the average Young's modulus for the undam-

aged specimen 1,635.96 ± 341.66 MPa compared with the hole-notched specimen, Young's modulus 1,450.41 ± 162.51 MPa. While for the elliptical-notched specimen the Young's modulus 710.06 ± 260.48 MPa as shown in Fig. 5(a), while Fig. 5(b) shows the average stresses for the three samples, which were 35.68 ± 8.60 MPa and for the undamaged specimen, and stress 21.28 ± 2.17 MPa and 12.81 ± 4.58 MPa for each of the hole-notched specimen and elliptical-notched specimens, respectively. Fig. 5(c) presents the deformation for the three samples. It showed less strain for the hole-notched specimen with an average strain of 2.16 ± 0.13%, followed by the elliptical-notched specimen with an average strain of 2.75 ± 0.65% and the largest of these was the undamaged specimen with an average strain of 3.68 ± 0.48% .The standard deviations of the three test samples for the undamaged specimen, the hole-notched specimen and the elliptical-notched specimen were in the range of 6%–37%.

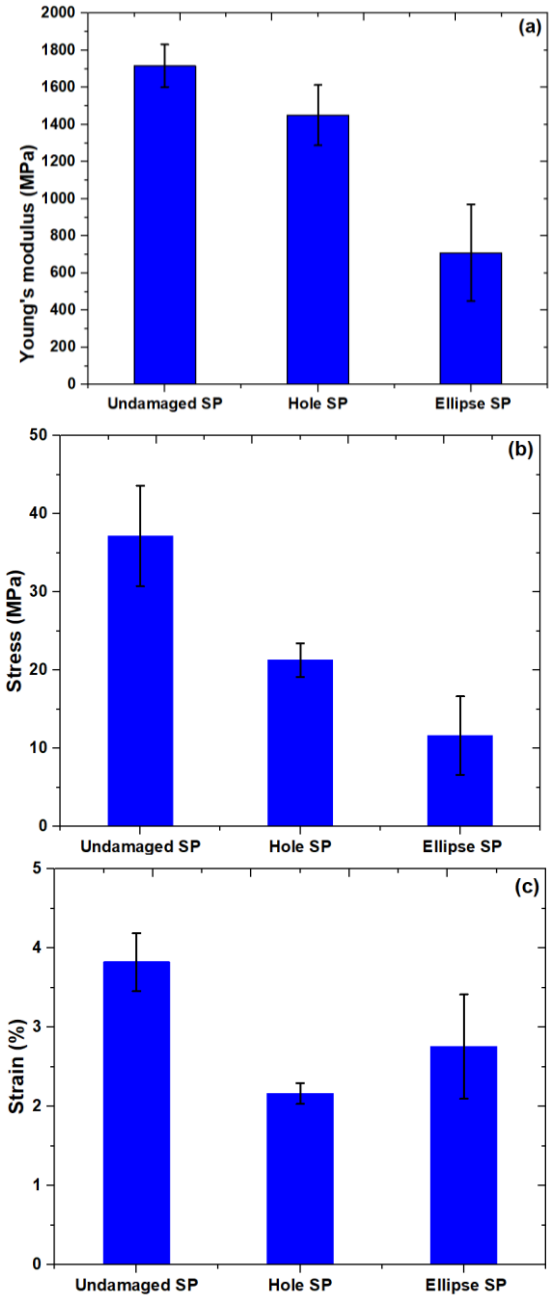

Fig. 5. Young's modulus and stress and strain for all three samples

4. NUMERICAL ANALYSIS

4.1. Mesh view

The numerical model was realised by FE under the code Abaqus. A fine mesh has been undertaken for the different models.

There are two types of mesh: a mesh around the hole and a uniform 3 × 3 mesh as shown in Fig. 6. The mesh around the circular hole and around the elliptical hole has been refined. The mesh optimisation provides accurate values compared with the normal mesh in the FEM, and thus gives better results to ensure convergence between the experimental and numerical results. They tried to model the three specimens with the same number of mesh elements, as shown in Fig. 6.

In order to be close to the real loading conditions in the traction machine, the following boundary conditions have been assumed. One end of the specimen was embedded and the other subjected to an applied stress. Application of force perpendicular force F = 1 mm/min to the tensile samples was done, as shown in Fig. 7.

Tab. 2. Input parameters of numerical simulation

Specimen	Total number of nodes	Displacement speed	Mesh type	Young's modulus (MPa)
Undamaged	1,008	1	Hexagon (C3D8R)	1,793.80
Hole-notched	1,050	1	Hexagon (C3D8R)	1,423.36
Elliptical-notched	1,050	1	Hexagon (C3D8R)	547.59

The tensile test of the specimens was carried out numerically and the behaviour of the specimens was studied according to the presence of the notch. In the numerical analysis in the ABAQUS software, it showed a convergence between the experimental results and the results of the numerical analysis for the three specimens (Figs 8–10). Moreover, the maximum stress value (red colour) was 41.20 MPa and the minimum stress (blue colour) was around 0 MPa for the undamaged specimen, as shown in Fig. 8. The maximum stress value (red colour) was 20.51 MPa and the minimum stress (blue colour) was around 0 MPa for the hole-notched specimen (Fig. 9). The maximum stress value (red colour) was 11.17 MPa and the minimum stress (blue colour) was around 0 MPa for the elliptical-notched specimen (Fig. 10).

A high concentration of stress is noted in the vicinity of the notch which reduces the resistance of the specimen. However, for the specimen without notch, the stresses are distributed uniformly along its useful length. The elliptical notch represents a higher concentration of stress than that in the presence of a circular notch. The stresses in the complete sample are greater than in the other samples. A comparison of the results was made with respect to the Young's modulus, maximum stress, and deformation between the experimental results and those obtained numerically (see Tab. 5). There is clearly a slight difference between the different properties between the simulation and experimental results.

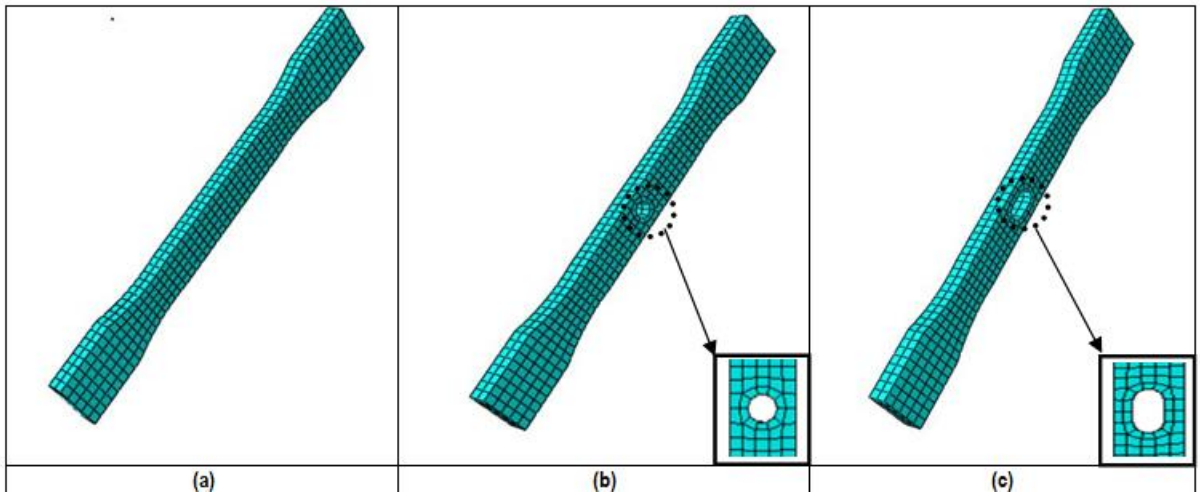

Fig. 6. Mesh view. (a) The undamaged specimen. (b) The hole-notched specimen. (c) The elliptical-notched specimen

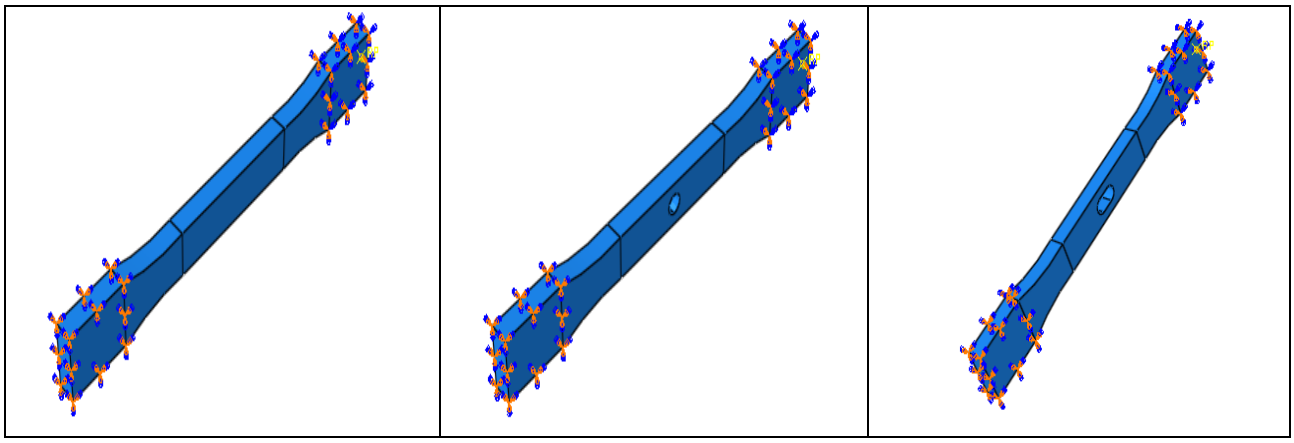

Fig. 7. Application of force to specimens in ABAQUS program

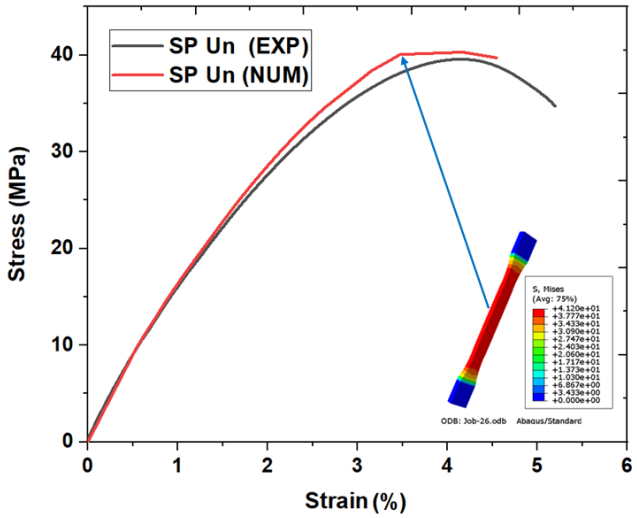

Fig. 8. Comparison between the experimental and numerical results for the undamaged specimen

It can be seen in Tab. 3 that the effect of stresses is higher in the undamaged specimen and lower in the elliptical-notched specimen. Stresses in the undamaged specimen were 41.20 MPa and stresses in the elliptical-notched specimen were 11.17 MPa. As for the results of PEMAG (the magnitude of equivalent plastic strains) and PEEQ (equivalent plastic strain) in the Abaqus software, the results were close and similar in the perforated and elliptical-notched specimen and slightly higher in the undamaged specimen.

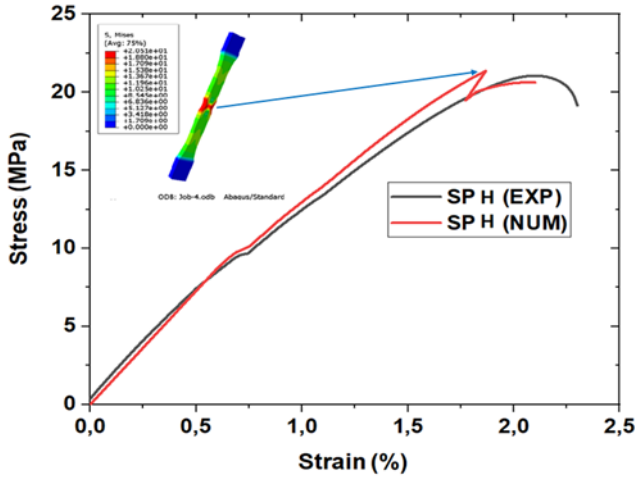

Fig. 9. Comparison between the experimental and numerical results for hole-notched specimen

Tab. 5 shows, comparing the results of the reactions generated in the three specimens along the steepest region, that the highest value of RF magnitude is 310.7 N in the undamaged

specimen, 83.49 N in the hole-notched specimen and 55.26 N in the elliptical-notched specimen. The displacement is close for the hole-notched specimen and the undamaged specimen of 5.993 mm and 4.580 mm, respectively, and it is lower for the elliptical-notched specimen of 1.421 mm.

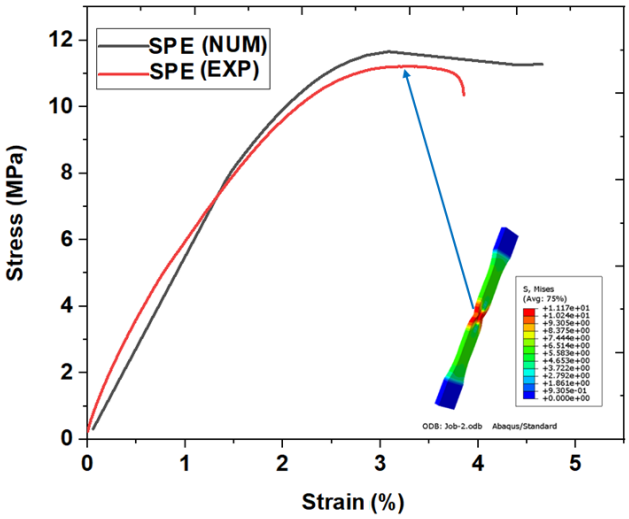

Fig. 10. Comparison between the experimental and numerical results for elliptical-notched specimen

Tab. 3. Experimental and simulation result with error for the stress

Specimen	Experimental	ABAQUS	Error (%)
Undamaged	41.20	41.22	0.04
Hole-notched	20.51	21.06	2 .61
Elliptical-notched	11.17	11.21	0.35

Tab. 4. Experimental and simulation result with error for the Young's modulus

Specimen	Experimental	ABAQUS	Error (%)
Undamaged	1,793.80	1,650.01	8.08
Hole-notched	1,423.36	1,185.92	16.89
Elliptical-notched	547.59	474.47	13.35

Fig. 11 shows that the cracks propagated directly from the edge of the hole to the nearest edge of the samples, due to the quasi-isotropic characteristic of the samples of the epoxy composites. This can be clearly seen in the optical images included in Fig. 11, the tensile specimens after fractures for all three types (undamaged, circular and elliptical). The damage occurred across the width of the specimen on either side of the hole at the notched specimen and the ellipse notched specimen, while different damage could be observed at various locations on solid specimens, the fracture of the destroyed specimen occurred along the plane perpendicular to the direction of maximum tensile stress.

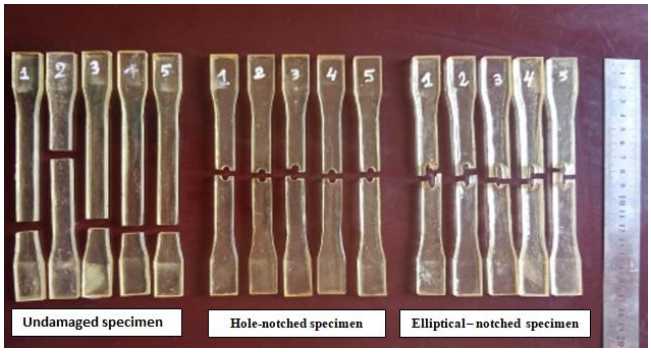

Fig. 11. Tensile specimens after fractures

Tab. 5. Comparison between numerical results for the three specimens on ABAQUS

Specimen	STRESS MAX (MPa)	E MAX(%) principal	PEMAG MAX (%)	PEEQ MAX	RF Magnitude MAX(N)	U Magnitude MAX(mm)	STATUSXFEM MAX
Undamaged	41.20	0.05828	0.03739	0.03740	310.7	4.580	1.000
Hole-notched	20.51	0.04016	0.02635	0.02640	83.49	5.993	1.000
Elliptical-notched	11.17	0.04185	0.02660	0.02660	55.26	1.421	0.4001
	STRESS min (MPa)	**E MIN (%) principal**	**PEMAG min (%)**	**PEEQ min**	**RF Magnitude min(N)**	**U Magnitude min(mm)**	**STATUSXFEM min**
Undamaged	3.333	4.86	0.003116	0.003116	25.89	0.3816	0.0800
Hole-notched	1.709	0.003347	0.002.196	0.002200	6.958	0.499	0.0833
Elliptical-notched	0.9305	0.003488	0.002261	0.0002217	4.602	0.1184	0.03334

5. CONCLUSION

The study undertaken in this work aims to use the XFEM technique for modelling the behaviour of an epoxy-type polymer to see the influence of the presence of notch on the tensile response. The obtained experimental results indicate that the undamaged specimen has ultimate tensile strength of 41.22 MPa and Young's modulus of 1,793.80 MPa, which are the strongest parts among the studied specimens. Comparison of the ultimate tensile strength indicates that an increase in hole diameter leads to a decrease in the strength of the part. The ultimate maximum stress is a decrease of 11.21 MPa and a Young's modulus of 547.59 MPa for the elliptical-notched specimen. The weakest examined is the elliptical-notched specimen. The standard deviations of the three test samples for the undamaged specimen, the

hole-notched specimen and the elliptical-notched specimen are in the range 6%–37%. The comparison of the numerical results with the experimental values revealed good agreement and that the error ratios are less than 3% for the maximum stress, while the error rate is less than 17% for the Young's modulus.

FE analysis using the XFEM technique is efficient and presents good results if the mesh of the specimen is well optimised.

A high stress concentration is noted around the elliptical and circular notches. These geometric discontinuities reduce the width of the plate and provide a considerable drop in the value of the maximum tensile stress.

REFERENCES

1. Hermansson F, Janssen M, Gellerstedt F. Environmental evaluation of Durapulp Bio-composite using LCA: comparison of two applications. J For. 2016; 5: 68-76.
2. Kahl S, Peng RL, Calmunger M, Olsson B, Johansson S. In situ EBSD during tensile test of aluminum AA3003 sheet. Micron. 2014. 58: 15-24.
3. Mohanty AK, Misra M, Drzal LT. Sustainable Bio-Composites from Renewable Resources: Opportunities and Challenges in the Green Materials World. J Polym Environ. 2002; 10(1): 19-26.
4. Calì M , Pascoletti G, Gaeta M , Milazzo G, Ambu R.A New Generation of Bio-Composite Thermoplastic Filaments for a More Sustainable Design of Parts Manufactured by FDM. Appl Sci. 2020; 10(17): 5852.
5. Paiva JMd, Mayer S, Rezende MC. Comparison of tensile strength of different carbon fabric reinforced epoxy composites. Mater Res. 2006; 9(1): 83-90.
6. Goutham ERS, Vamshi Y, Namratha M, Gupta KB, Chandrasekar M, Naveen J. Influence of glass fibre hybridization on the open hole tensile properties of pineapple leaf fiber/epoxy composites. AIP Conf Proc;2022.
7. Larbi Chaht F, Mokhtari M, Benzaama H. Using a Hashin Criteria to predict the Damage of composite notched plate under traction and torsion behavior. Frat.Integrità.Strut. 2019; 13(50): 331-341.
8. SaadallahY Modeling of mechanical behavior of cork in compression. Frat.Integrità.Strut.2020; 14(53): 417-425.
9. Huang Y, Frings P, Hennes E. Mechanical properties of Zylon/epoxy composite. Composites, Part B.2002; 33(2): 109-115.
10. Duc F, Bourban PE, Månson JAE The role of twist and crimp on the vibration behaviour of flax fibre composites. Compos Sci Technol 2014; 102: 94-99.
11. uillén-Rujano R, Avilés F, Vidal-Lesso A, Hernández-Pérez A.Closed-form solution and analysis of the plate twist test in sandwich and laminated composites. Mech Mater. 2021; 155: 103753.
12. Tretyakova TV, Wildemann VE, Strungar EM. Deformation and failure of carbon fiber composite specimens with embedded defects during tension-torsion test. Frat.Integrità.Strut .2018; 12(46):295-305.
13. Liang S, Gning PB, Guillaumat L.A comparative study of fatigue behaviour of flax/epoxy and glass/epoxy composites. Compos Sci Technol. 2012; 72(5): 535-543.
14. Lu Z , Feng B, Loh C.Fatigue behaviour and mean stress effect of thermoplastic polymers and composites. Frat Integrità Strut 2018;12(46): 150-157.
15. Banaszkiewicz M, Dudda W. Applicability of notch stress-strain correction methods to low-cycle fatigue life prediction of turbine rotors subjected to thermomechanical loads. acta mech autom. 2018;12(3).
16. Panettieri E, Fanteria D , Montemurro M . Low-velocity impact tests on carbon/epoxy composite laminates: A benchmark study. Compos B Eng. 2016;107: 9-21.
17. Baykan BM, Yolum U , Özaslan E , Güler MA, Yıldırım B. Failure Prediction of Composite Open Hole Tensile Test Specimens Using Bond Based Peridynamic Theory. Procedia Struct Integ. 2020; 28: 2055-2064.
18. Hao A, Zhao H, Chen JY. Kenaf/polypropylene nonwoven composites: The influence of manufacturing conditions on mechanical, thermal, and acoustical performance. Compos B Eng. 2013; 54: 44-51.
19. Galeta T, Raos P , Stojšić J , Pakši I. Influence of Structure on Mechanical Properties of 3D Printed Objects. Procedia Eng. 2016; 149: 100-104.
20. hosravani MR, Rezaei S , Faroughi S , Reinicke T. Experimental and numerical investigations of the fracture in 3D-printed open-hole plates. Theor Appl Fract Mech.2022; 121:103543.
21. Zako M, Uetsuji Y, Kurashiki T. Finite element analysis of damaged woven fabric composite materials. Compos Sci Technol. 2003; 63(3):507-516.
22. Dixit A, Mali HS. Modeling techniques for predicting the mechanical properties of woven-fabric textile composites: a review. Mech compos Mater. 2013; 49(1): 1-20.
23. Eshraghi S, Das S. Micromechanical finite-element modeling and experimental characterization of the compressive mechanical properties of polycaprolactone–hydroxyapatite composite scaffolds prepared by selective laser sintering for bone tissue engineering. Acta biomater. 2012; 8(8): 3138-3143.
24. Mohammadi R , Najafabadi MA, Saeedifar M . Correlation of acoustic emission with finite element predicted damages in open-hole tensile laminated composites. Compos B Eng. 2017; 108: 427-435.
25. Ghezzo, F, Giannini G, Cesari F, Caligiana G, Numerical and experimental analysis of the interaction between two notches in carbon fibre laminates. Compos Sci Technol. 2008; 68(3): 1057-1072.
26. Liao T, Adanur S. A Novel Approach to Three-Dimensional Modeling of Interlaced Fabric Structures. Text Res J. 1998; 68(11): 841-847.
27. Bogrekci I, Demircioglu P, Sucuoglu HS,Altun E, Sakar B, Durakbasa MN, Topology Optimization of a Tensiletest Specimen. Int Sci Bk; 2020.
28. Khosravani MR. Influences of defects on the performance of adhesively bonded sandwich joints. Key eng mater; 2018.
29. Kojnoková T, Nový F, Markovičová L. Evaluation of tensile properties of carbon fiber reinforced polymers produced from commercial prepregs. Mater Today Proc. 2022; 62: 2663-2668.
30. Xu P, Yang C, Peng Y , Yao S, Zhang D, Li B .Crash performance and multi-objective optimization of a gradual energy-absorbing structure for subway vehicles. int j mech sci. 2016; 107:1-12.
31. Feulvarch E, Lacroix R, Deschanels H, A 3D locking-free XFEM formulation for the von Mises elasto-plastic analysis of cracks. Comput Methods Appl Mech Eng. 2020; 361: 112805.
32. Frolov AS, Fedotov IV, Gurovich BA. Evaluation of the true-strength characteristics for isotropic materials using ring tensile test. nucl eng technol. 2021; 53(7): 2323-2333.
33. Pilkey WD, Pilkey DF, Bi Z. Peterson's stress concentration factors;2020.

Khalissa Saada: https://orcid.org/0000-0002-3025-1287

Salah Amroune: https://orcid.org/0000-0002-9565-1935

Moussa Zaoui: https://orcid.org/0009-0005-7178-2542

Amin Houari: https://orcid.org/0009-0004-2617-2182

Kouider Madani: https://orcid.org/0000-0003-3277-1187

Amina Hachaichi: https://orcid.org/0000-0002-4905-7599